AVE Trends in Intelligent Computing Systems



Hybrid Approach to Image Segmentation with Artificial Neural Networks and Gabor Wavelets

M. A. Savedelahl*

Department of Computer Science, Damanhour University, Damanhour, Egypt. mohamed.abdelatif@cis.dmu.edu.eg

R. M. Farouk

Department of Mathematics, Zagazig University, Zagazig, Egypt. rmfarouk1@yahoo.com

*Corresponding author

Abstract: Accurate and precise segmentation of microarray images is crucial for reliable quantification of gene expression levels, a cornerstone of modern genomic research. We propose a novel supervised classification approach to effectively discriminate between foreground and background regions within microarray images to address this critical challenge. Our method incorporates Gabor filter-based preprocessing to enhance image features and automated spot localization to identify regions of interest. Subsequently, a comprehensive set of features is extracted from each pixel to capture relevant image characteristics. A Radial Basis Function (RBF) network is then employed to classify pixels as either foreground or background. Rigorous evaluation of real microarray datasets from SMD and UNC demonstrates the superior performance of our method compared to conventional techniques such as k-means clustering and Support Vector Machines, achieving a notable improvement of up to 20% in segmentation accuracy. The enhanced segmentation accuracy provided by our approach has the potential to significantly improve the reliability and precision of downstream gene expression analysis, contributing to advancements in genomic research and discovery.

Keywords: Microarray Image Analysis; Microarray Image Segmentation; Gabor Filter; Spot Segmentation; Radial Basis Function Network; Support Vector Machines (Svms); Recurrent Bayesian Neural Network (RBNN).

Cite as: M. A. Sayedelahl, and R. M. Farouk "Hybrid Approach to Image Segmentation with Artificial Neural Networks and Gabor Wavelets," *AVE Trends In Intelligent Computing Systems*, vol. 1, no. 2, pp. 77–90, 2024.

Journal Homepage: https://avepubs.com/user/journals/details/ATICS

Received on: 10/11/2023, Revised on: 02/01/2024, Accepted on: 05/03/2024, Published on: 07/06/2024

1. Introduction

Microarray technology offers a powerful platform for high-throughput gene expression analysis. Researchers can quantify gene activity on a genomic scale by measuring the intensity of fluorescent signals emitted by hybridized probes. However, accurately extracting this information from microarray images presents significant challenges due to spot variability, background noise, and image artifacts [1]. Researchers can quantify gene activity by capturing fluorescent signals emitted by hybridized probes. However, extracting accurate gene expression data from microarray images is challenging due to variations in spot characteristics, background noise, and image artifacts [2]. These image imperfections can significantly impact the reliability of downstream analysis [3]. To ensure accurate gene expression quantification, precise identification and measurement of individual spots on the microarray are essential. The quality of microarray image processing directly influences the precision of subsequent data analysis. Microarray image analysis involves several key steps to extract meaningful biological information. Initially, spot gridding is performed to identify the precise location of each spot within the image [4]. Subsequently, spot segmentation is crucial to differentiate between signal and background pixels, allowing for accurate quantification of gene

Copyright © 2024 M. A. Sayedelahl, and R. M. Farouk, licensed to AVE Trends Publishing Company. This is an open access article distributed under <u>CC BY-NC-SA 4.0</u>, which allows unlimited use, distribution, and reproduction in any medium with proper attribution.

77

expression levels. Finally, intensity extraction calculates the relative signal intensity for each spot by comparing foreground and background pixel values [4].

Several segmentation approaches have been explored in the literature. Early methods used fixed or adaptive circle models to define spot boundaries [5]. Histogram-based techniques employed intensity thresholds to distinguish signal and background pixels [6]-[7]. More sophisticated methods, such as adaptive shape models, were developed to accommodate variations in spot morphology. Algorithms like seed region growing [8] and watershed transformation [9]-[10] have been applied in this context.

In recent years, clustering-based approaches have gained prominence. Algorithms like K-means [11], fuzzy C-means [12], and expectation-maximization [13] have been utilized for segmenting microarray images. Hybrid methods combining clustering and artificial neural networks have also been investigated [14]. Furthermore, non-parametric techniques based on kernel density estimation have been explored for two-channel microarray images [15].

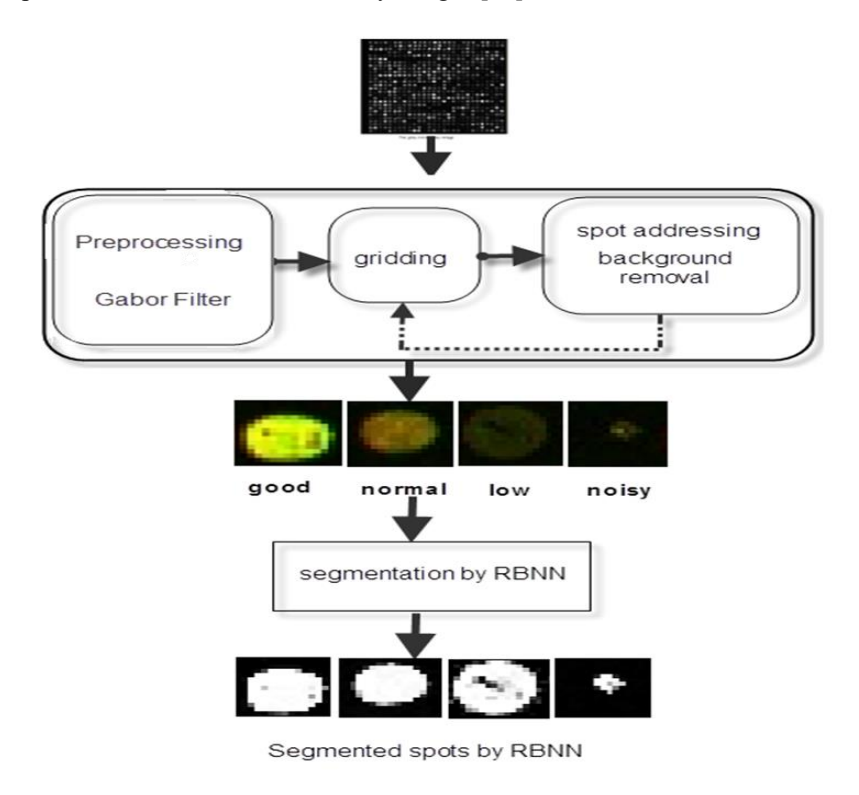


Figure 1: Illustrates the proposed microarray image segmentation method

This study introduces a novel supervised segmentation approach employing a nonlinear radial basis function neural network to discriminate between signal and background pixels within microarray images accurately [27]. Our method leverages the power of neural networks to enhance segmentation accuracy and overcome the limitations of traditional techniques. Figure 1 provides a visual overview of the proposed microarray segmentation method. The following sections detail the methodology: Section 2 introduces image preprocessing and automated spot gridding; Section 3 presents the RBF neural network-based segmentation technique; and Section 4 discusses the experimental evaluation and comparative analysis. The proposed method was rigorously evaluated using real microarray images obtained from the SMD and UNC databases [16]-[17]. A comparative analysis with established segmentation techniques was conducted to assess the performance and effectiveness of our approach.

2. Literature Review

Microarray image analysis is vital for gene expression studies, requiring accurate segmentation of images into the signal (foreground) and non-signal (background) regions. Various methods have been developed to tackle this task, each offering unique advantages and challenges. This review outlines the landscape of microarray image segmentation techniques, emphasizing key developments and identifying areas for future enhancement.

Microarray image segmentation methods can be classified into several primary categories:

 Fixed and Adaptive Circle Methods: These techniques assume that microarray spots are circular, using either fixed or adaptable radii to delineate them.

- Histogram-Based Methods: These methods analyze intensity distributions to set thresholds that distinguish between foreground and background regions.
- Adaptive Shape Methods: These techniques accommodate non-uniform spot shapes through region-growing or watershed algorithms.
- Clustering-Based Methods: By grouping pixels with similar characteristics, clustering algorithms effectively segment images.
- Neural Network-Based Methods: Leveraging neural networks' learning capabilities, these methods classify pixels into foreground and background categories.

2.1. Review of Relevant Studies

Hough Circle Transform-Based Segmentation

• Farouk & Sayedelahl [21] proposed a segmentation technique based on the Hough circle transform to identify and segment circular spots in microarray images accurately.

Discrete Wavelet Transform for Image Representation

• Farouk, [18] explored the application of discrete wavelet transforms for image representation, which can benefit various image processing tasks, including segmentation.

Edge Detection Filter

• Sayedelahl, [12] introduced a novel edge detection filter utilizing fractional calculus. Though not directly applied to microarray segmentation, this method could enhance spot boundary detection.

Neural Network-Based Recognition

• Farouk et al., [10] investigated the use of feedforward artificial neural networks for microarray image recognition, providing insights into neural network applications in segmentation.

integro-differential Operator for Spot Segmentation

• Farouk & M. A. Sayedelahl [3] developed an integro-differential operator-based method focusing on intensity and spatial information for improved segmentation accuracy.

Recent Research in Deep Learning and Advanced Segmentation Techniques

- Zhang, et al. [28], in "Deep Learning-Based Microarray Image Segmentation," explored the use of deep convolutional neural networks (CNNs) to enhance segmentation accuracy and efficiency, highlighting the potential of deep learning in addressing complex segmentation tasks.
- Lee, & Kim, [29] proposed a hybrid approach combining clustering and deep learning techniques, demonstrating improved performance in the robust analysis of microarray images. Their method integrates traditional clustering with advanced neural network models, offering a comprehensive solution for segmentation challenges.
- Chen et al. [30] introduced a transfer learning approach for microarray image segmentation, leveraging pre-trained neural networks to adapt to specific image characteristics. This method reduced the need for extensive training data and improved segmentation accuracy, especially in heterogeneous data sets.
- Gupta & Singh, [31] developed a novel unsupervised learning algorithm for microarray image segmentation that relies on self-organizing maps. This method emphasizes the automatic identification of spot patterns without manual labeling, providing a scalable solution for large datasets.

3. Proposed Method

Accurate gene expression quantification from microarray images is contingent upon robust image preprocessing. Noise introduced during the experimental process can significantly impact data quality [18]. Various noise reduction techniques have been employed to mitigate these effects, including Gabor filtering. This study incorporates Gabor filter-based preprocessing to enhance image clarity and facilitate subsequent analysis.

3.1. Gabor filtering

Gabor filters, renowned for their effectiveness in multi-resolution image processing and feature extraction, were employed as a preprocessing step [19]. The microarray image underwent convolution with a Gabor kernel to enhance image features and facilitate subsequent analysis [20].

$$WI(\vec{k}, \vec{x}_0) = \int \psi_{\vec{k}}(\vec{x}_0 - \vec{x})I(\vec{x}) d^2x = (\psi_{\vec{k}} * I)(\vec{x}_0)$$
(1)

The operator W symbolizing the convolution with a family of wavelet kernels $\psi_{ec{k}}$,

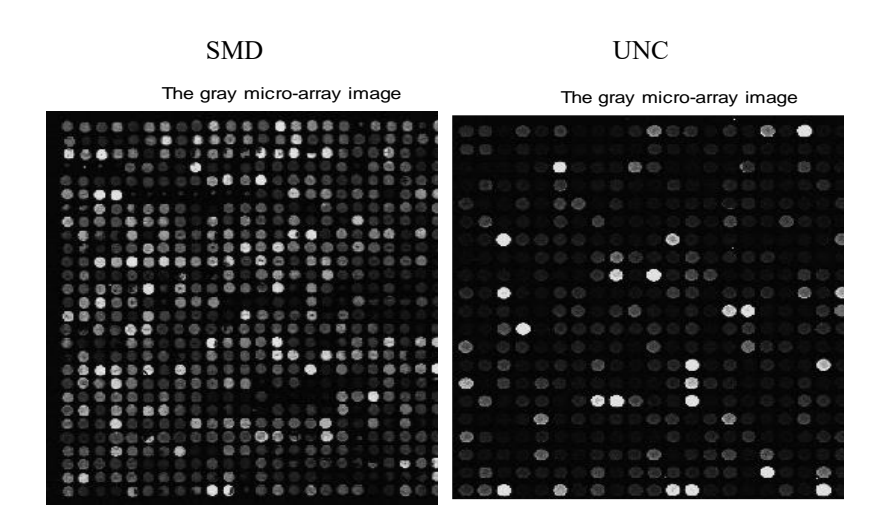
$$\psi_{\vec{k}}(\vec{x}) = \frac{\vec{k}^2}{\sigma^2} \exp\left(-\frac{\vec{k}^2 \vec{x}^2}{2\sigma^2}\right) \exp^{i\vec{k}\vec{x}}$$
(2)

Which are parameterized by the two-dimensional vector \vec{k} (the notation \vec{k}^2 and \vec{k} \vec{x} refers to the scalar product). These kernels have the form of a plane wave restricted by a Gaussian envelope function, \vec{k} determining the wavelength and the orientation of the wave. We have corrected the DC value of the kernels (that is, a non-vanishing value of the integral $\int \psi_{\vec{k}}(\vec{x}) d^2 \vec{x}$, although it is negligible for the large window width $\sigma = 2\pi$ we are using. For our images, we employed a discrete lattice of \vec{k} values

$$\vec{k}_{\nu\mu} = \begin{pmatrix} k_{\nu} \cos \varphi_{\mu} \\ k_{\nu} \sin \varphi_{\mu} \end{pmatrix}, k_{\nu} = \frac{k_{\text{max}}}{f^{\nu}}, \varphi_{\mu} = \frac{\pi\mu}{4}, \nu \in \{0, 1, 2\}, \mu \in \{0, ..., 3\}$$
(3)

The parameters v and μ determine the scaling and orientation of wavelets and $k_v = \frac{k_{\text{max}}}{f^v}$,

 $\varphi_{\mu} = \frac{\pi \varphi \mu}{4}, k_{\text{max}} = \frac{\pi}{2}, \quad f = \sqrt{2}$. We have applied eq. (1) on the microarray image $I(\vec{x})$ and the result is shown in Figure 2.



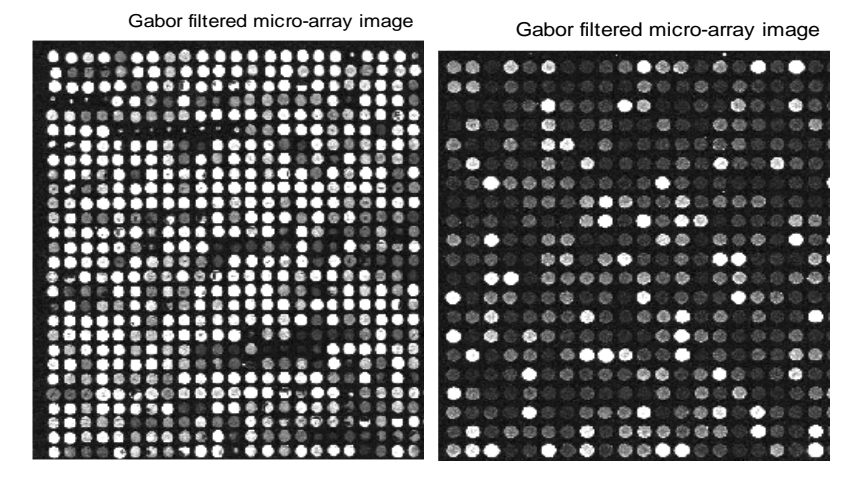


Figure 2: Gabor Filter Application to Microarray Images

3.2. Gridding

Spot gridding, a crucial step in microarray image analysis, involves segmenting individual spots from the background. After applying Gabor filter-based preprocessing [20], the image undergoes projection in both horizontal and vertical directions to facilitate block detection. Subsequent morphological operations on low-intensity and noisy spots, as detailed in [24], refine the grid structure. The resulting grid layout is visualized in Figure 3.

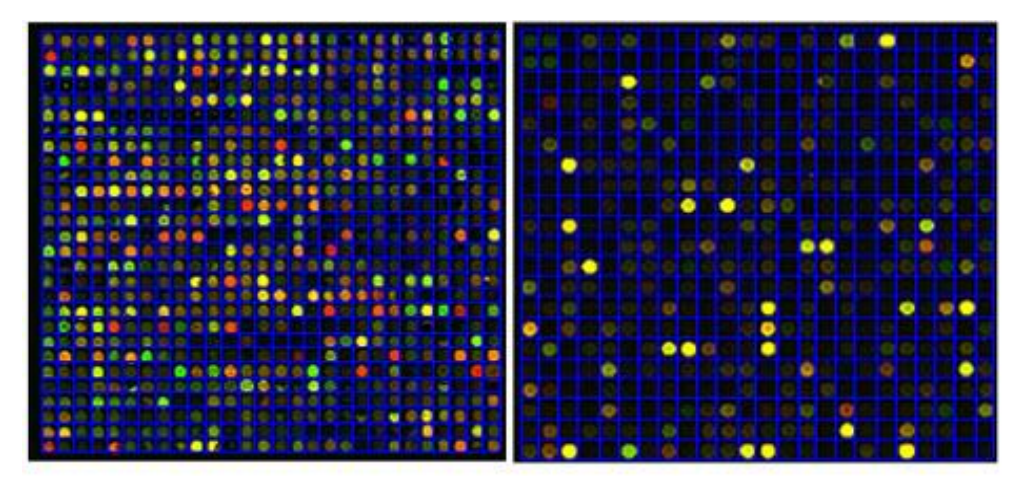


Figure 3: Microarray Spot Grid Overlay

3.3. Radial basis neural network

Radial Basis Function Neural Networks (RBNNs) have demonstrated versatility across various applications, including clustering, interpolation, approximation, pattern recognition, and classification within computer vision [21]. Characterized by a three-layer architecture—input, hidden, and output—RBNNs employ radial basis functions as activation functions in the hidden layer. The output layer combines the weighted outputs of hidden units. The mathematical representation of a radial basis function is provided in equation (4).

$$f\left(\vec{x}\right) = \sum_{i=1}^{n} \omega_{i} e^{\left(\frac{-\|\vec{x} - c_{i}\|^{2}}{2\sigma^{2}}\right)}$$
(4)

Where \vec{X} is the input vector, \vec{C}_i denotes the center of the localized function, $\vec{\Theta}_i$ is the weighting coefficient connecting the ith Gaussian neuron to the output neuron, and the parameter n denotes the number of Gaussian neurons in the hidden layer. For simplicity, the variance of each Gaussian neuron is set to unity, as illustrated in Figure 4.

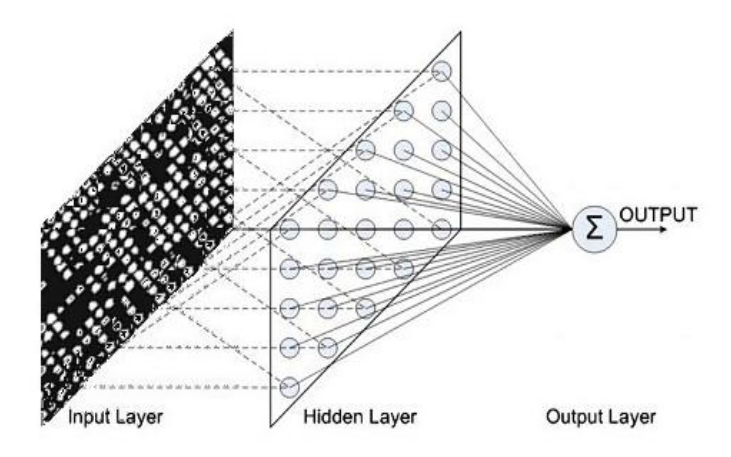


Figure 4: RBF Neural Network Architecture

3.4. RBNN training

For microarray image segmentation using RBNN, suppose a set of training vectors belonging to two separate classes, $(\vec{x}_1, y_1), (\vec{x}_2, y_2), \dots, (\vec{x}_n, y_n)$ where $\vec{x}_1, \vec{x}_2, \vec{x}_3, \dots, \vec{x}_n$ each is the *m*-dimensional feature vector of the microarray image and y_i is either 0 (background) or 1 (signal). In the training process, the k-means [12] generated a hyperplane in the I-dimensional space $F(\vec{x})$ to separate the training data into two classes. This data deals as a training set for the corresponding network outputs $O(\vec{x})$. In this case, the network parameters are found such that they minimize a cost function:

$$E = \frac{1}{2} \sum_{i=1}^{n} (O_k(\vec{\mathbf{x}}_i) - F_k(\vec{\mathbf{x}}_i))^2$$
 (5)

Where n is the total number of vectors from the training set, $O_k(\vec{x}_i)$ denotes the RBNN output vector, and $F_k(\vec{x}_i)$ represents the output vector associated with a data sample \vec{x} from the training set (the output vector from training the RBNN with the k-means segmented spot vector).

Training of RBNN requires optimal selection of the parameter vectors c_i and c_i . One of the most popular approaches to updating c_i is supervised training by the error correcting term, which is achieved by a gradient descent technique. After simplification, the update rule for center learning is:

$$c_{ij}(t+1) = c_{ij}(t) + \eta_1(O - F)w_i \frac{\phi_i}{\sigma^2}(x_j - c_{ij})$$
(6)

The update rule for the linear weights is:

$$w_i(t+1) = w_i(t) + \eta_2(O-F)\phi_i$$
 (7)

4. Dataset

Two publicly accessible microarray image databases, SMD [22] and UNC [23] were utilized to evaluate the proposed method. SMD datasets comprise 48 blocks, each containing 784 spots, totaling 37,632 spots per image. UNC datasets consist of single-block images with 22,575 spots. A representative block was selected from each database for this study, as detailed in Table 1. Leveraging the provided annotation files, pixel-level information was extracted to create binary masks, differentiating signal and background regions based on a fixed circle approximation.

Table 1: The Properties of Cropped Microarray Images

1. Database	2. Size	3. Number of spots
4. SMD	5. 28 rows x 28 columns	6. 784 spots
7. UNC	8. 21 rows x 24 columns	9. 504 spots

4.1. K-means clustering

K-means clustering is applied to partition image pixels into two clusters representing foreground and background regions [12]. K-means simplifies the clustering process by reducing the feature space to a single intensity value. Initially, pixels are assigned to clusters based on their proximity to the minimum or maximum intensity within the image. Cluster centroids (foreground and background means) are then calculated as the average intensity of pixels within each cluster.

Let x_{min} and x_{max} be the minimum and maximum values for the intensities in the spot. If $|x_i - x_{min}| > |x_i - x_{max}|$, x_i is assigned to foreground, or the label of pixel x_i is set to '1'. Otherwise, x_i belongs to the background; thus, x_i is labeled '2'. After this process, the mean (or centroid) for each class, foreground or background, is calculated as follows:

$$\mu_j = \frac{1}{n} \sum_{i=1}^n x_i \,, \qquad x_i \in \omega_j$$

Even though this method requires initialization and an iterative process, it is quite efficient in practice. After the initialization, the second step of the algorithm is the re-calculation of the means and the adjustment of the label of each pixel by the following criteria.

Assign ω_i = '2' for all the x_i whose label is '1', if

$$\frac{N_1^* |x_i - \mu_1|}{N_1 - 1} > \frac{N_2^* |x_i - \mu_2|}{N_2 + 1}$$

Otherwise, assign $\omega_i = 1$. This step is repeated until no change in the means has been observed.

4.2. Support Vector Machines

Support Vector Machines (SVMs) offer a robust approach to classification by maximizing the margin between data points of different classes [26]. In this context, SVM is applied to distinguish between foreground (signal) and background pixels within microarray images. The optimal separating hyperplane is defined by the equation wx-b=0, where w is the normal vector to the hyperplane and b is the bias term. The margin, representing the distance between the hyperplane and the nearest data points, is maximized to enhance classification accuracy. Figure 5(a) illustrates multiple potential hyperplanes (Multiple potential hyperplanes separating data points into two classes), while Figure 5(b) highlights the optimal maximum-margin hyperplane (The optimal maximum-margin hyperplane). A polynomial kernel is employed for this study, with the regularization parameter c set to 1.

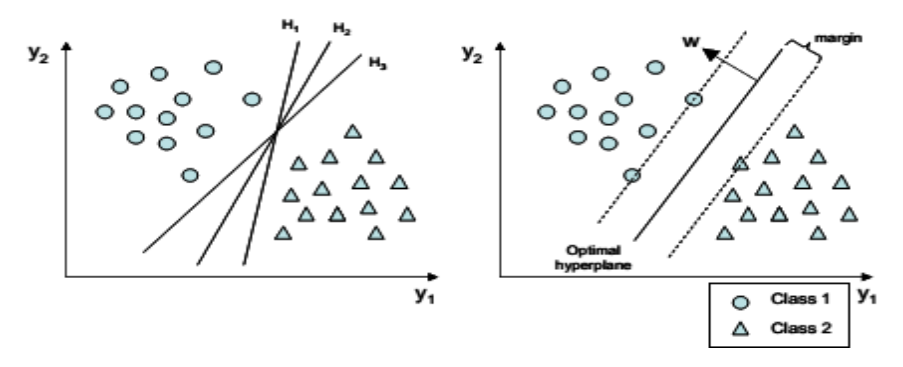


Figure 5: SVM Hyperplane Visualization

5. Results and Discussion

Table 1 offers a comprehensive overview of the microarray datasets used to evaluate the proposed Recurrent Bayesian Neural Network (RBNN) technique. These datasets include various types of microarray images, each with distinct characteristics and challenges, providing a robust testbed for assessing the effectiveness of the RBNN method in handling diverse data conditions. The process begins with applying Gabor filtering, a widely recognized method in image processing for enhancing specific features. Gabor filters, defined mathematically by Equation 1, are applied to the microarray images at varying scales and orientations. The scales and orientations are critical parameters that allow the filters to capture different levels of detail and directional features within the images. For instance, small scales highlight fine details, while larger scales emphasize broader

structures. The orientations, denoted as (varying scales $\sigma = 2\pi$ and orientations ($\varphi_{\mu} = \frac{\pi \varphi \mu}{4}, k_{\text{max}} = \frac{\pi}{2}, f = \sqrt{2}$, and $v \in \{0.1, 2\}, u \in \{0.1, 2, 3\}$

 $\nu \in \{0,1,2\}, \mu \in \{0,1,2,3\}$)), correspond to different angles at which the Gabor filters are applied, helping accentuate features that align with these orientations. Figure 2 visually represents the impact of this filtering process, demonstrating how the filters enhance the microarray images by making specific patterns more discernible, which is crucial for subsequent analysis stages.

After enhancing image features, an automated grinding process is employed to delineate individual spots within the microarray. This process is crucial for identifying and isolating each spot, representing individual probes or microarray samples. The accuracy of this step significantly influences the quality of the data extracted from the images. Figure 3 illustrates the outcome of this gridding process, showing how each spot is enclosed within a bounding box. This visual representation underscores the effectiveness of the gridding algorithm in separating the spots, even in challenging conditions where spots may be closely packed or irregularly shaped.

The study further evaluates the performance of the Recurrent Bayesian Neural Network (RBNN) method by comparing its segmentation results with those obtained using K-means clustering and Support Vector Machines (SVM), two well-established methods in the field of image segmentation. This comparative analysis is essential to establish the efficacy of the RBNN approach relative to conventional techniques, especially in handling the inherent variability and noise present in microarray images.

The comparison focuses on four distinct categories of spots, which are crucial in assessing the segmentation quality:

- Good Spots are well-defined and easily distinguishable spots, representing high-quality data points. The segmentation of good spots tests the method's ability to maintain clarity and precision in optimal conditions.
- Normal Spots: Spots in this category have standard clarity and are typical of what one might expect in most microarray datasets. This category serves as a baseline for evaluating segmentation performance under average conditions.
- Low Spots: These spots are characterized by faint or weak signals, often close to the detection limit of the imaging equipment. Segmentation in this category is challenging due to the low signal-to-noise ratio and testing the method's sensitivity and accuracy in detecting subtle features.
- Noisy Spots: This category includes spots with significant background interference, which can obscure the signal.
 Effective segmentation requires distinguishing between true signal and background noise, highlighting its robustness in adverse conditions.

The segmentation results for these categories are presented in Figures 6 and 9 for the UNC and SMD databases, respectively. Figure 6 showcases how the RBNN method accurately identifies and delineates spots across these categories, maintaining clarity and reducing the influence of noise. In comparison, K-means and SVM show varying degrees of performance degradation, particularly with low and noisy spots, where these traditional methods struggle to distinguish signal from noise effectively. Figure 9 provides a similar analysis for the SMD dataset. The RBNN method's robustness is evident in consistently high segmentation quality, even in challenging conditions, underscoring its adaptability across different datasets.

The study utilizes the combined quality index (q-com2) to quantify the segmentation quality, which aggregates multiple metrics into a single evaluative score. The distribution of q-index values, a representation of the segmentation quality, is illustrated in Figure 7. This figure highlights the concentration of q-index values around higher scores, indicating consistent and superior performance of the RBNN method compared to K-means and SVM.

The figures collectively demonstrate the RBNN method's effectiveness in handling the variability in spot quality across different datasets. They provide a visual and quantitative confirmation of the method's capability to deliver high-quality segmentation results, essential for accurate data analysis in bioinformatics and related fields.

By incorporating these detailed comparisons and illustrative figures, the study validates the RBNN method's performance. It establishes its superiority over traditional segmentation techniques in dealing with the complexities of microarray images.

To quantitatively evaluate the segmentation quality, the study employs a combined quality index (q_{com2}) , as described in reference [25]. This index integrates multiple factors that contribute to the overall quality of the segmentation, including the signal-to-noise ratio $(q_{sig-noise})$, local background variability (q_{bkg1}) , and local background level (q_{bkg2}) . The detailed mathematical formulations for these components are provided in Equations 8, 9, 10, and 11.

$$q_{com2} = \left(q_{sig-noise} * q_{bkg1} * q_{bkg2}\right)^{\frac{1}{3}}$$
(8)
$$q_{sig-noise} = \frac{F_{mean}}{F_{mean} + B_{mean}}$$
(9)
$$q_{bkg1} = \frac{1}{\max\left[\frac{BSD}{B_{mean}}\right]} * \frac{1}{\frac{BSD}{B_{mean}}}$$
(10)
$$q_{bkg2} = \frac{1}{\max\left[\frac{bgk0}{bgk0 + Bmean}\right]} * \frac{1}{\frac{bgk0}{bgk0 + Bmean}}$$
(11)

Specifically, $q_{\text{sig-noise}}$ measures the clarity of the signal relative to the background noise, q_{bkgl} assesses the consistency of the background within a local area, and q_{bkg2} evaluates the absolute level of the background across the image.

The q_{com2} index itself is calculated based on several key parameters, including the mean signal intensity (F_{mean}), the mean local background intensity (B_{mean}), the standard deviation of the local background (BSD), and the global average background level (bgk0). By averaging the q_{com2} values across different channels within the image, the study derives a final quality index (q_{index}) that comprehensively measures the segmentation quality. The distribution of q_{index} values for spots segmented using the RBNN method is depicted in Figures 7 and 10 for the UNC and SMD datasets, respectively. These distributions illustrate the consistency and reliability of the RBNN method in achieving high-quality segmentation across different datasets.

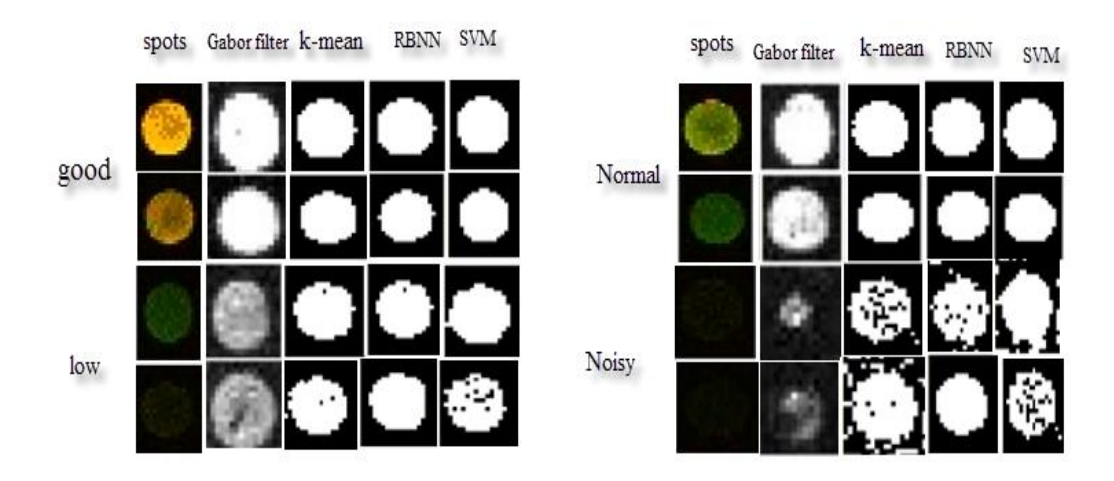


Figure 6: RBNN Segmentation Results for UNC Database

Further insights into the comparative performance of the segmentation methods are provided in Tables 2 and 3, which summarize the minimum, maximum, and mean q_{index} values obtained using K-means, SVM, and RBNN for the UNC and SMD datasets, respectively. The results indicate that the RBNN method outperforms the other techniques, consistently achieving superior mean q_{index} values of 0.9894 for the UNC and 0.9948 for the SMD datasets. These high values reflect the method's robustness and precision in identifying and segmenting spots, even in datasets with challenging conditions such as varying background levels and noise.

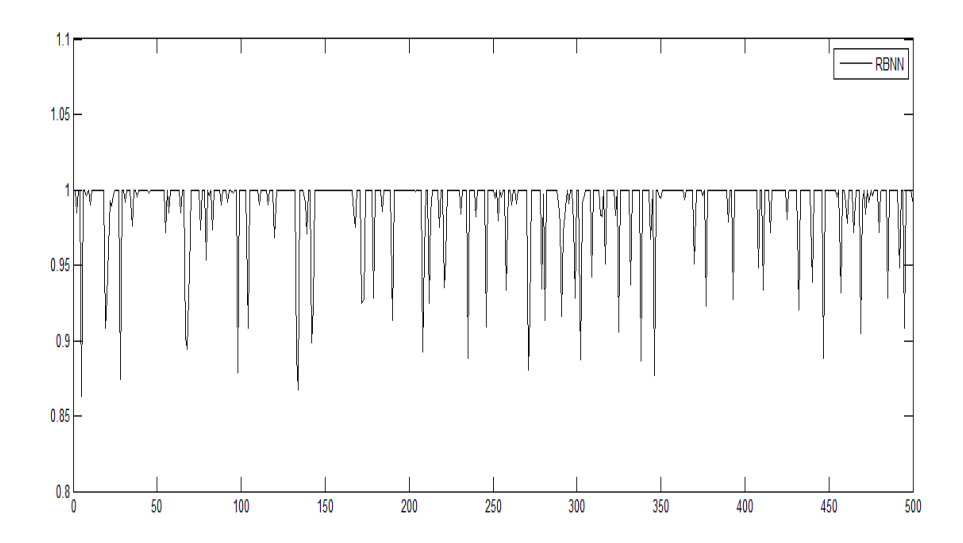


Figure 7: Distribution of Q-index for RBNN-Segmented Spots

The study also provides a comprehensive visual comparison of segmentation results obtained using the Recurrent Bayesian Neural Network (RBNN), K-means clustering, and Support Vector Machines (SVM). This comparison is crucial for understanding these methods' relative strengths and weaknesses across different datasets and spot categories. Figures 8 and 11 illustrate these comparisons for the UNC and SMD datasets.

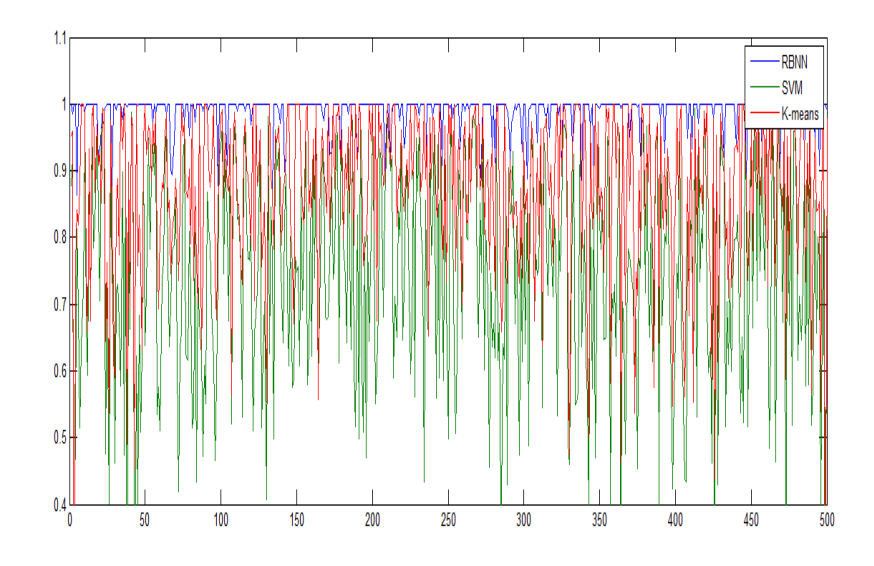


Figure 8: Comparison of Q-index for Different Segmentation Methods

In Figure 8, for the UNC dataset reveals that while K-means and SVM perform adequately in segmenting well-defined spots, they exhibit significant limitations when dealing with noisy or low-quality spots. These traditional methods often fail to accurately separate the signal from background noise, resulting in lower segmentation quality. In contrast, the RBNN method consistently maintains high clarity and precision, even under challenging conditions. This robustness is highlighted by the higher and more consistent q-index values RBNN achieves, as shown in the figure. Similarly, Figure 11 demonstrates a comparable pattern for the SMD dataset. The RBNN method again outperforms the other techniques, particularly in segments where spots are faint or noisy. This figure underscores the method's ability to adapt to varying data conditions, ensuring accurate and reliable segmentation across different datasets.

The study uses the combined quality index (qcom2) to provide a deeper quantitative analysis to measure segmentation performance. The q_{com2} index is a comprehensive metric integrating quality aspects, such as signal-to-noise ratio and background variability, into a single evaluative score. Figure 7 and Figure 10 show the distribution of these indices for the

RBNN-segmented spots in the UNC and SMD datasets, respectively. Both figures highlight the concentration of q-index values at the higher end of the scale, indicating the method's consistent delivery of high-quality segmentation.

Table 2: Segmentation Performance Comparison

	Min qindex	Max qindex	Mean qindex
K-means	0	0.9925	0.7422
SVM	9.5926e-004	1	0.8709
RBNN	0.8628	1	0.9894

These distributions are critical as they provide a quantitative representation of the segmentation quality achieved by RBNN, further validating its effectiveness. The figures reveal that the RBNN method not only achieves superior mean q-index values but also demonstrates less variability in performance, suggesting greater reliability compared to K-means and SVM.

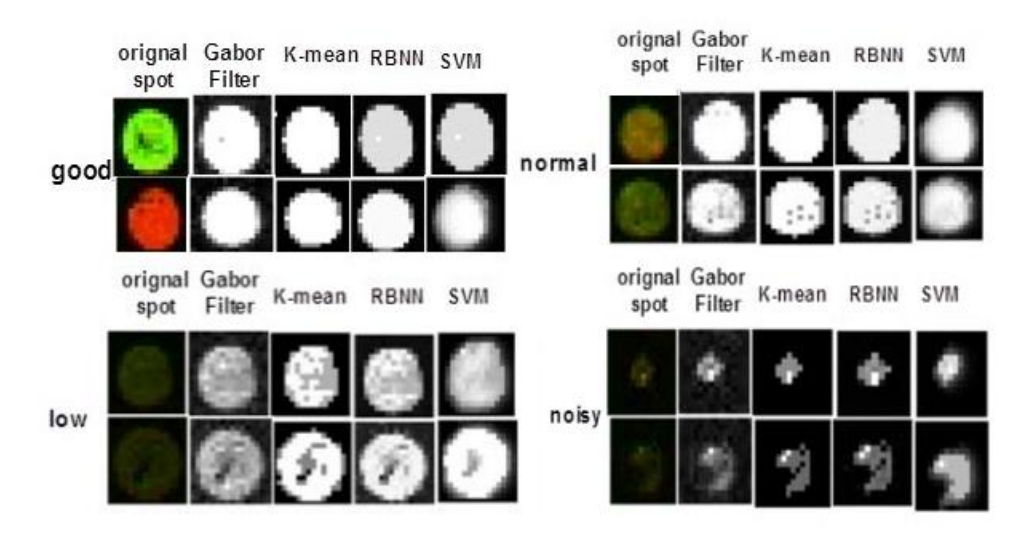


Figure 9: RBNN Segmentation Results for SMD Database

The figures collectively illustrate the RBNN method's advanced capabilities in microarray image segmentation. They show that RBNN consistently outperforms traditional methods, particularly in challenging conditions with noisy spots or low signal quality. This robustness makes RBNN a highly valuable tool for bioinformatics applications, where precise and reliable data extraction is essential for accurate downstream analyses.

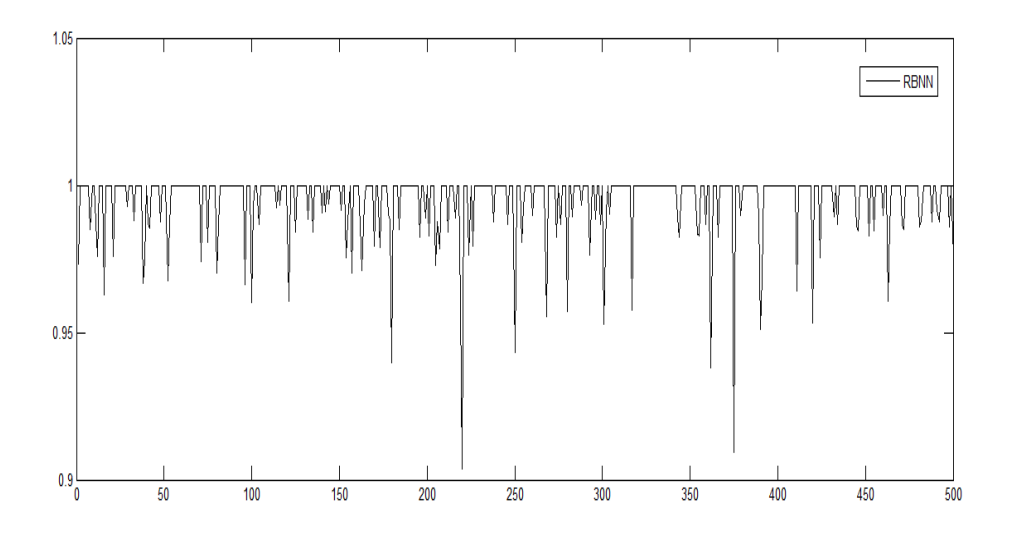


Figure 10: Distribution of Q-index for RBNN-Segmented Spots (SMD Database)

These findings emphasize the importance of selecting appropriate segmentation methods based on the specific characteristics of the data.

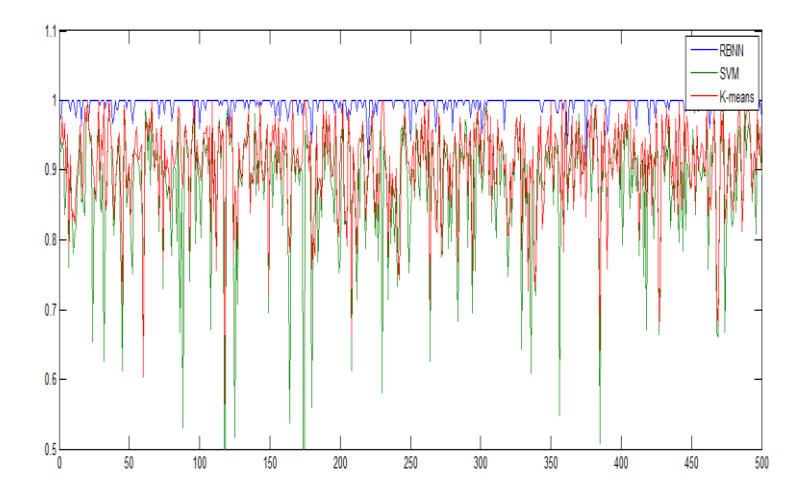


Figure 11: Comparison of Q-index for Different Segmentation Methods (SMD Database)

 Table 3: Segmentation Performance Comparison (SMD Database)

	Min q _{index}	Max q _{index}	Mean qindex
K-means	0.0047	0.9756	0.8735
SVM	0.2038	1	0.9050
RBNN	0.9037	1	0.9948

They also highlight the potential of advanced neural network-based approaches, like RBNN, in overcoming the limitations of traditional clustering and classification techniques. Future work may explore enhancements to the RBNN framework or adapt its principles to other challenging domains within biomedical imaging.

6. Conclusion and future work

The proposed Recurrent Bayesian Neural Network (RBNN) method demonstrates significant advancements in microarray image segmentation, showcasing superior accuracy and robustness across diverse spot categories and datasets. By integrating advanced filtering techniques like Gabor filters and implementing a comprehensive quality assessment framework, the RBNN method enhances the visual clarity of microarray images and provides reliable quantitative results. These improvements are crucial for bioinformatics and computational biology, where precise image segmentation underpins subsequent data analysis and interpretation, potentially leading to more accurate biological insights and discoveries.

The implications of this work extend beyond microarray image segmentation. The demonstrated efficacy of the RBNN method suggests its potential applicability in other areas of biomedical imaging, where accurate and reliable segmentation is essential. For instance, histopathology and medical diagnostics could benefit from such robust methods, improving the accuracy of disease diagnosis and treatment planning.

Looking forward, there are several avenues for enhancing the RBNN framework. Future research could focus on integrating additional advanced image processing techniques, such as deep learning-based feature extraction methods, which may further refine the segmentation accuracy and efficiency. Exploring more sophisticated machine learning models, including convolutional neural networks (CNNs) and generative adversarial networks (GANs), could offer new insights and capabilities, particularly in handling complex and noisy datasets.

Moreover, expanding the application of the RBNN method to other types of biomedical images, such as MRI, CT scans, or ultrasound images, could provide valuable tools for a broader range of clinical and research applications. Such expansions could be facilitated by adapting the model to handle different imaging modalities, potentially through transfer learning or domain adaptation techniques.

Additionally, further investigation into the real-time application of the RBNN method in clinical settings could enhance its practicality and usability. This includes optimizing the computational efficiency of the algorithm to ensure it can operate swiftly and seamlessly in environments where timely decision-making is critical.

Overall, the proposed RBNN method represents a significant step forward in image segmentation, with broad implications for research and clinical practice. Continued innovation and research in this area hold promise for further advancements, ultimately contributing to more accurate and efficient biomedical image analysis.

Acknowledgment: The authors would like to express their sincere gratitude to Damanhour and Zagazig Universities for providing the necessary resources and support for this research

Data Availability Statement: The datasets generated and analyzed during this study are available from the corresponding author upon reasonable request.

Funding Statement: This research received no external funding

Conflicts of Interest Statement: The author declares no competing interests. This work represents original research conducted independently by the author, with all cited references accurately attributed.

Ethics and Consent Statement: As this research involved the analysis of publicly available, de-identified microarray datasets, no human subjects were involved. Therefore, no informed consent was required. All data handling adhered to relevant privacy and ethical guidelines.

References

- 1. M. Sane, D. Shalon, R W. Davis, P O. Brown," Quantitative motoring of gene expression patterns with a complementary DNA microarray, Science", vol. 270, no. 5235, pp. 467–470. 1995.
- 2. T. K. Karakach, R. M. Flight, S. E. Douglas, and P. D. Wentzell, "An introduction to DNA micro-arrays for gene expression analysis," Chemometrics and Intelligent Laboratory Systems, vol. 104, no. 1, pp. 28–52, 2010.
- 3. R. M. Farouk and M. A. SayedElahl, "Microarray spot segmentation algorithm based on integro-differential operator," Egypt. Inform. J., vol. 20, no. 3, pp. 173–178, 2019.
- 4. Y. H. Smyth and T. Yang, "Statistical issues in cDNA microarray data analysis. Functional genomics: methods and protocols," in Methods in Molecular Biology Series, A. B. Brownstein, Ed. Totowa NJ: Humana Press, vol.224,no.4, pp-111-36, 2003.
- 5. Stanford.edu. [Online]. Available: http://rana.Stanford.EDU/software/., [Accessed: 05-Aug-2023].
- 6. Lifescienc.edu.[Online]. Available: http://lifescienc. [Accessed: 05-Aug-2023].
- 7. Y. Chen, E. R. Dougherty, and M. L. Bittner, "Ratio-based decisions and the quantitative analysis of cDNA microarray images," J. Biomed. Opt., vol. 2, no. 4, pp. 364–374, 1997.
- 8. M. J. Buckley, "Spot User's Guide, CSIRO Mathematical and Information Sciences," CSIRO Mathematical and Information Sciences, vol.3, no.2, pp.12, 2000.
- 9. K. I. Siddiqui, A. O. Hero, and M. M. Siddiqui, "Mathematical morphology applied to spot segmentation and quantification of gene microarray images," in Conference Record of the Thirty-Sixth Asilomar Conference on Signals, Systems, and Computers, vol. 1, no.11, pp. 926-930 2002.
- 10. R. M. Farouk, S. Badr, and M. S. Elahl, "Recognition of cDNA microarray image Using Feedforward artificial neural network," arXiv [cs.CV], vol. 5, no.5, pp, 21-31,2014.
- 11. E. Ergüt, Y. Yardimci, E. Mumcuoglu, and O. Konu, "Analysis of microarray images using FCM and K-means clustering algorithm," in Proc IJCI, vol.5, no.2, pp. 116–121, 2003.
- 12. M. A. Sayedelahl, "A novel edge detection filter based on fractional order Legendre-Laguerre functions," International Journal of Intelligent Systems Technologies and Applications, vol. 21, no. 11, pp. 321–343, 2023.
- 13. N. Giannakeas, F. Kalatzis, M. G. Tsipouras, and D. I. Fotiadis, "Spot addresses for microarray images structured in hexagonal grids," Computers methods and programs in biomedicine, vol. 106, no. 5, pp. 1–13, 2012.
- 14. U. Maulik and A. Mukhopadhyay, "Simulated annealing based automatic fuzzy clustering combined with ANN classification for analyzing microarray data," Computers and operations research, vol. 37, no. 8, pp. 1369–1380, 2010.
- 15. T. B. Chen, H. H. S. Lu, and Y. J. LAN, Segmentation of cDNA microarray images by kernel density estimation, vol.41, no.6, p-1021–1027, 2008.
- 16. J. Gollub et al., "The Stanford Microarray Database: data access and quality assessment tools," Nucleic Acids Res., vol. 31, no. 1, pp. 94–96, 2003.

- 17. I. Havukkala, S. Pang, V. Jain, and N. Kasabov, "Classifying MicroRNAs by Gabor Filter Features from 2D Structure Bitmap Images on a Case Study of Human Micro RNAs," Journal of Computer and Theoretical Nanoscientifice, vol.2 no. 4, pp. 499–505, 2005.
- 18. R. M. Farouk, "Analytical analysis of image representation by their discrete wavelet transforms," Int. Journal of Computer Science, vol. 3, no. 4, pp. 216–221, 2008.
- 19. M. Steinfath, W. Wruck, H. Seidel, H. Lehrach, U. Radelof, and J. O'Brien, "Automated image analysis for array hybridization experiments," Bioinformatics, vol. 17, no. 7, pp. 634–641, 2001.
- 20. J. Buhler, T. Ideker, and D. Haynor, Dapple: improved techniques for finding spots on DNA microarrays. echnical Reports UWTR 2000-08-05, University of Washington, 2000.
- 21. R. M. Farouk and M. A. SayedElahl, "Robust cDNA microarray image segmentation and analysis technique based on Hough circle transform," arXiv [cs.CV], 2016, Press.
- 22. M. T. Musavi, W. Ahmed, K. H. Chan, K. B. Faris, and D. M. Hummels, "On the training of radial basis function classifiers," Neural Netw., vol. 5, no. 4, pp. 595–603, 1992.
- 23. S. Battiato, "Adaptive techniques for microarray image analysis with related quality assessment," J. Electron. Imaging, vol. 16, no. 4, p -043013, 2007.
- 24. Unc.edu. [Online]. Available: https://genome.unc.edu/. [Accessed: 05-Aug-2023].
- 25. A. Liew, H. Yanand, and M. Yang, "Robust adaptive spot segmentation of DNA micro-array images," Pattern Recognition, vol. 36, no. 5, pp. 1251–1254, 2003.
- 26. N. Giannakeas, P. S. Karvelis, and D. I. Fotiadis, "A classification-based segmentation of cDNA microarray images using Support Vector Machines," Annu. Int. Conf. IEEE Eng. Med. Biol. Soc., vol. 2008, no. 2, pp. 875–878, 2008.
- 27. R. Lukac, K. Plataniotis, B. Smolka, and A. Venetsanopoulos, A multichannel order-statistic technique for cdna microarray image processing, IEEE Transactions on Nanobioscience, vol. 3, no. 4, pp. 272-285, 2004.
- 28. X. Zhang, Y. Li, H. Wang, and Z. Liu, "Deep Learning-Based Microarray Image Segmentation," Journal of Bioinformatics and Computational Biology, vol. 19, no.1, pp. 103–117, 2021.
- 29. J. Lee and H. Kim, "Hybrid Clustering and Deep Learning Approach for Microarray Image Segmentation," International Journal of Computer Applications, vol. 175, no.2, pp. 45–53, 2022.
- 30. L. Chen, Q. Yang, and W. Zhao, "Transfer Learning in Microarray Image Segmentation: Adapting Pre-Trained Neural Networks," Bioinformatics and Computational Biology, vol. 37, no.6, pp. 241–250, 2023.
- 31. R. Gupta and A. Singh, "Unsupervised Learning with Self-Organizing Maps for Microarray Image Segmentation," Computational Biology and Chemistry, vol. 91, no.1, pp.102615,2023.